64 Vaughan-Jones, R.D., Lederer, W.J., and Eisner, D.A., Ca^{2+} ions can affect intracellular pH in mammalian cardiac muscle. Nature, Lond. *301* (1983) 522–524.
65 Vercesi, A., Reynafarje, B., and Lehninger, A.L., Stoichiometry of H^+ ejection and Ca^{2+} uptake coupled to electron transport in rat heart mitochondria. J. biol. Chem. *253* (1978) 6379–6385.
66 Warner, A.E., Guthrie, S.C., and Gilula, N.B., Antibodies to gap-junctional protein selectively disrupt junctional communication in the early amphibian embryo. Nature, Lond. *311* (1984) 127–131.
67 Weidmann, S., The electrical constants of Purkinje fibres. J. Physiol. *118* (1952) 348–360.
68 Weidmann, S., The diffusion of radiopotassium across intercalated disks of mammalian cardiac muscle. J. Physiol. *187* (1966) 323–342.
69 Weidmann, S., Electrical coupling between myocardial cells, in: Progress in Brain Research, vol. 31, pp. 275–281. Eds K. Akert and P.G. Waser. Elsevier, Amsterdam 1969.
70 Weingart, R., The actions of ouabain on intercellular coupling and conduction velocity in mammalian ventricular muscle. J. Physiol. *264* (1977) 341–365.
71 Weingart, R., Hess, P., and Reber, W.R., Influence of intracellular pH on cell-to-cell coupling in sheep Purkinje fibers, in: Normal and Abnormal Conduction in the Heart, pp. 73–84. Eds A.P. de Carhalho, B.F. Hoffman and M. Lieberman. Futura, New York 1982.
72 Wojtczak, J., Contractures and increase in internal longitudinal resistance of cow ventricular muscle induced by hypoxia. Circ. Res. *44* (1979) 88–95.
73 Wojtczak, J., Influence of cyclic nucleotides on the internal longitudinal resistance and contractures in the normal and hypoxic mammalian cardiac muscle. J. molec. cell. Cardiol. *14* (1982) 259–265.

0014-4754/87/101084-08$1.50 + 0.20/0

Cell-to-cell coupling studied in isolated ventricular cell pairs

by R. Weingart and P. Maurer

Department of Physiology, University of Berne, Bühlplatz 5, 3012 Berne (Switzerland)

Summary. Cell pairs isolated from adult rat and guinea pig ventricles were used to study the electrical properties of the nexal membrane. Each cell of a pair was connected to a voltage-clamp system so as to enable whole-cell, tight-seal recording. The current-voltage relationship of the nexal membrane was found to be linear, revealing a resistance r_n of 2–4 MΩ. r_n was insensitive to the sarcolemmal membrane potential (range: −90 to +30 mV), and exerted no time-dependent gating behavior (range: 0.1 to 10 s). Lowering pH_i yielded a small increase in r_n. Vigorous elevations in $[Ca^{2+}]_i$ gave rise to an increase in r_n which was associated with a cell shortening. Uncoupling caused by aliphatic alcohols or halothane did not produce cell shortening. Cell pairs were also used to study action potential transfer.
Key words. Myocytes; electrical coupling; cell-to-cell coupling; nexus.

Introduction

Since the pioneering work of Weidmann[15], cable analysis has been used extensively in cardiac tissue to study the electrical properties involved in intercellular coupling[4]. This approach revealed quantitative information about the overall intracellular resistance pathway (r_i) which consists of the repetitive arrangement of two resistive elements in series, the cytoplasm (r_c), and the nexal membrane (r_n). However, a major limitation of cable analysis has been that the structure responsible for intercellular communication, i.e. the nexal membrane, is not accessible *directly* to a functional investigation.

With the introduction of novel methods such as enzymatic procedures for isolating cells, and recording techniques suitable for small cells[11], the situation changed fundamentally. Utilizing isolated cardiac cell pairs in conjunction with patch-clamp pipettes, it became feasible to explore the electrical properties of the nexal membrane itself.

Methods

Figure 1A shows the experimental arrangement[17] adopted. Each cell of a cell pair was connected to a patch-clamp pipette so as to enable tight-seal, whole-cell recording. A double voltage-clamp method was employed which allowed one to control the membrane potential of cell 1 (V_1) and cell 2 (V_2) individually. The associated currents flowing through each pipette were measured separately (I_1 and I_2). Figure 1B shows the equivalent circuit used for the analysis. It includes three resistive elements: $r_{m,1}$ and $r_{m,2}$, the resistances of the sarcolemmal membrane of cell 1 and cell 2; and r_n, the resistance of the nexal membrane.

According to this model, current injected into a pipette flows via either of two pathways, a) directly through r_m of the injected cell, or b) via r_n through r_m of the other cell. Thus, in general the pipette current represents the sum of two current components, which, however, under appropriate conditions may be separated. This is possible when voltage-clamp pulses are applied to one of the cells, while the other cell remains at the common holding potential, V_H. In this case, the voltage

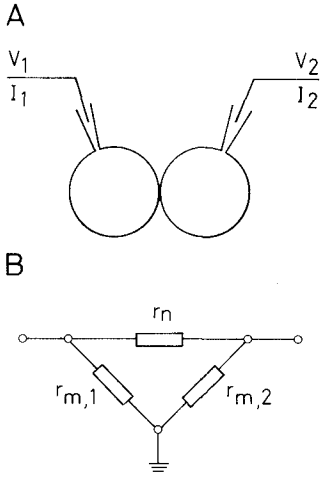

Figure 1. *A* Diagram of the experimental arrangement. Each cell of a cell pair was connected to a patch-clamp pipette. Separate voltage-clamp circuits enabled us to apply voltage steps (V_1, V_2) to each cell and to measure the resulting currents (I_1, I_2) individually. *B* Equivalent circuit used to analyze the data. It consists of $r_{m,1}$ and $r_{m,2}$, the resistances of the sarcolemmal membranes of cell 1 and cell 2, and r_n, the resistance of the nexal membrane. From Weingart[17].

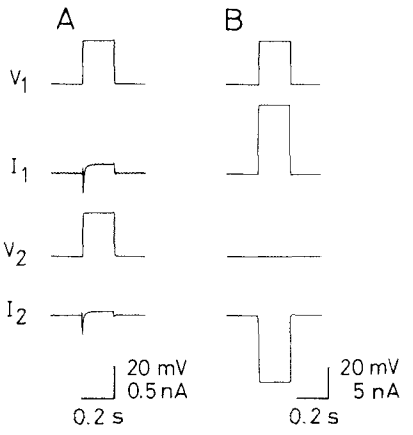

Figure 2. Current flow in a cell pair under voltage-clamp condition. *A* Symmetrical pulse application. A clamp pulse (+27 mV, 200 ms; $V_H = -42$ mV) was administered to cell 1 (V_1) and cell 2 (V_2) simultaneously. The resulting current signals I_1 and I_2 showed a time-dependent inward current surge. *B* Asymmetrical pulse application. A pulse identical to that in *A* was applied to cell 1 (V_1), while the membrane potential of cell 2 remained constant. The associated current records displayed large time-independent signals. From Weingart[17].

step applied to the pulsed cell corresponds to the voltage gradient across the nexal membrane, V_n, while the pipette current of the non-pulsed cell represents the nexal membrane current, I_n. Utilizing these two quantities, we can determine the basic electrical properties of the nexal membrane.

Results

a) Basic electrical properties

Applying the double voltage-clamp approach to a cell pair, two different pulse protocols may be adopted. Figure 2A illustrates the case involving a symmetrical pulse protocol. Starting from a V_H of −42 mV, an identical voltage-clamp pulse (+27 mV, 200 ms) was administered to both cells simultaneously, in such a way that there was no voltage gradient across the nexal membrane. The associated current signals, I_1 and I_2, reflect current flowing across the sarcolemmal membranes of cells 1 and 2. At the beginning of the pulse, time-dependent Ca^{2+}-inward current surges developed, which were followed by steady K^+-outward currents. Such current responses may be obtained irrespective of whether the cells investigated are electrically coupled or not. Thus, this protocol does not yield information about intercellular coupling. Figure 2B illustrates the case involving an asymmetrical pulse protocol; i.e., the same voltage-clamp pulse as before was now applied to cell 1, while cell 2 remained at the common V_H. This protocol produced large current signals exerting a different time course. According to figure 1, I_1 reflects the sum of two current components, one a small time-dependent current flowing across $r_{m,1}$, identical to I_1 in figure 2A, and the other a large time-independent current flowing across r_n. I_2 on the other hand corresponds to the current required to prevent cell 2 from being depolarized. Its amplitude equals the current flowing across the nexal membrane. Therefore, the asymmetrical pulse protocol represents a useful approach to study the electrical properties of the nexal membrane.

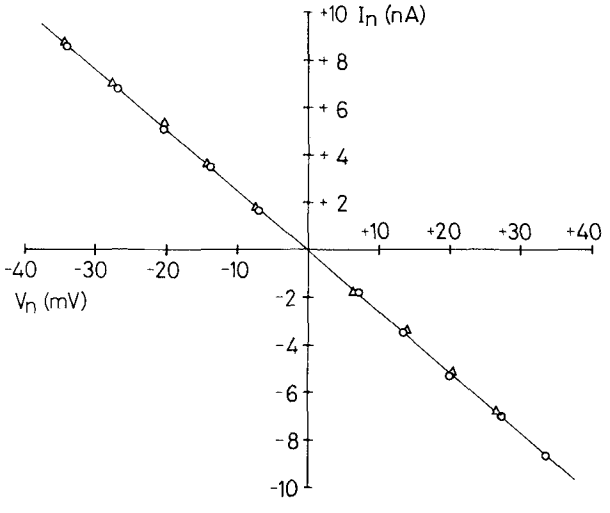

Figure 3. Steady-state current-voltage relationship of the nexal membrane. The plot of nexal membrane current I_n versus nexal membrane voltage V_n revealed a linear behavior, no matter whether cell 1 (o) was pulsed or cell 2 (△). Regression analysis revealed an r_n of 3.25 MΩ for the pooled data points. From Weingart[17].

Initially, we investigated the current-voltage relationship of the nexal membrane making use of the following protocol. A voltage-clamp pulse of variable amplitude and either polarity was applied first to cell 1 and then to cell 2, while the associated nexal current was measured. The analysis of a representative experiment of this kind is illustrated in figure 3.

It shows a plot of the nexal membrane current I_n, (current measured from the non-pulsed cell) versus the transjunctional voltage gradient V_n (voltage step applied to the pulsed cell). The circles and triangles represent individual data points for the cases where cell 1 and cell 2, respectively, were pulsed. The slope of the current-voltage relationship yielded a r_n of 3.25 MΩ. Thus, the nexal membrane exerts an ohmic resistance and does not discriminate between the directions of current flow.

As indicated in the table, values of r_n determined in this manner ranged from 2 to 4 MΩ. The table lists additional parameters pertinent to cell-to-cell coupling which may be derived from r_n and morphometrical data. If we assume a nexal membrane area per cell pair of 5.16 μm^2 [12], and a hexagon spacing of 10.25 nm^2, the number of connexons turns out to be 60.000. Therefore, the specific nexal membrane resistance, R_n, is calculated to be 0.1–0.2 Ωcm^2, and the conductance of a single connexon 5–10 pS.

Thus, at the membrane level, the nexal membrane resistivity is 4–5 orders of magnitude lower than the non-junctional membrane resistivity[6]. This finding is in agreement with the results previously obtained from intact cardiac tissue[16]. At the single-channel level, the connexon conductance seems to be comparable to the conductance of a Ca^{2+}-channel[13]. This finding is surprising in view of data obtained with other methods. For example, diffusion studies revealed a cut-off limit for nexal membrane permeation of about 1000 daltons[5] and thus predict an effective pore diameter of 1–1.5 nm. Such a pore (diameter = 1–1.5 nm; length = 200 nm), filled with 150 mmol/l KCl solution (conductivity = 58Ωcm), exerts a conductance of 70–150 pS. Furthermore, single-channel measurements performed in our laboratory (unpublished) and others[7, 14] revealed a connexon conductance of 40–150 pS. There are at least two reasons as to why the connexon conductance inferred from the r_n measurements is much lower. It is conceivable that the morphometrical data derived from intact ventricular muscle is not adequate for isolated cell pairs. More attractively, only a fraction of connexons may be in operation at any given time.

At that point, the question arises whether r_n is affected by the sarcolemmal membrane potential or not. This problem has been explored employing the following pulse protocol. A

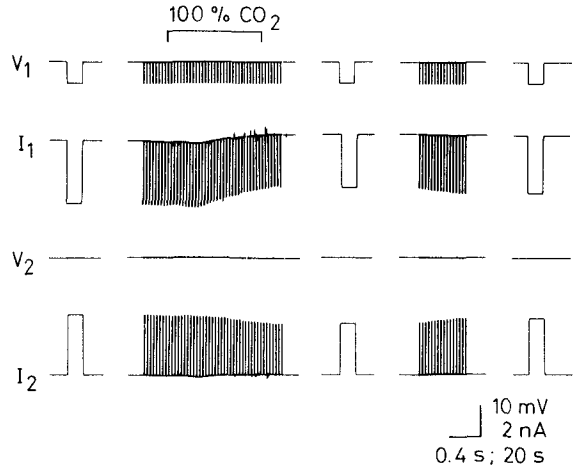

Figure 4. Effect of CO_2 on intercellular coupling. A voltage-clamp pulse (−7 mV; 200 ms; V_H = −42 mV) was applied to cell 1 (V_1) at a frequency of 0.3 Hz. The figure shows a continuous recording of the four standard signals monitored, the voltages and currents from cell 1 (V_1, I_1) and cell 2 (V_2, I_2). For clarity, signals corresponding to control, peak effect, and re-control, have been displayed on an expanded time scale (see insets). As judged from the observed change in nexal membrane current I_2, intracellular acidification gave rise to a reversible increase in r_n of 13%.

standard clamp pulse (+25 mV; 200 ms) was applied consecutively to cell 1 and cell 2, superimposed on a common but varying V_H. This protocol enabled us to determine r_n as a function of the non-junctional membrane potential. It turned out that r_n was insensitive to V_m over the voltage range covered by a cardiac action potential, i.e. from −90 mV to +30 mV.

Another interesting problem concerns putative changes in r_n as a function of time. To explore this possibility, voltage-clamp pulses of variable duration were applied to one cell of a cell pair, while the transmembrane voltage of the other cell was maintained at the V_H. Varying the pulse duration from 0.1–10 s, we could not detect any signs of a time-dependent gating mechanism.

b) Modification of r_n

Studies performed on intact cardiac preparations have demonstrated that r_n may be modified under certain experimental

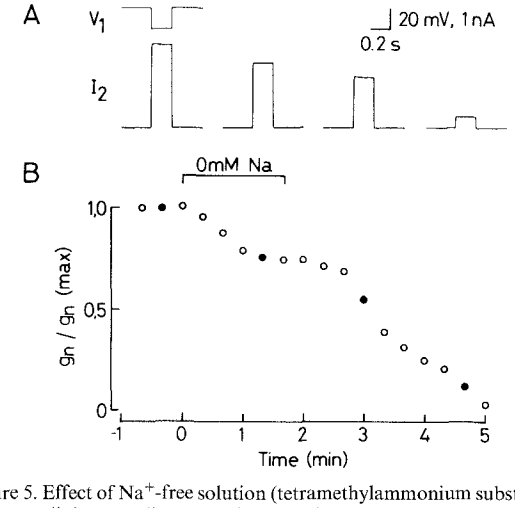

Figure 5. Effect of Na^+-free solution (tetramethylammonium substituted) on intercellular coupling. *A* Selected voltage-clamp records. A clamp pulse (−20 mV, 200 ms; V_H = −68 mV) was applied to cell 1 (V_1) and the associated nexal current measured (I_2). *B* Analysis of the experimental data. Values of g_n were normalized and plotted versus time. The filled circles correspond to the values calculated from the records shown in (*A*).

Basic electrical properties of the nexal membrane of mammalian ventricular muscle.

Nexal membrane properties		Reference
Nexal membrane resistance	2–4MΩ	8, 17
Nexal membrane area	5.16 μm^2	12
Connexon spacing	10.25 nm	2
Connexons/cell pair	60.000	
Specific nexal membrane resistance	0.1–0.2 Ωcm^2	17
Single connexon conductance	5–10 pS	17

conditions. The relevant conditions involve interventions aimed at elevating the $[H^+]_i$[10], or $[Ca^{2+}]_i$[3], and exposure to aliphatic alcohols[2], or anesthetics[18]. Working with cardiac cell pairs, we made use of different interventions in order to explore their effects on r_n[8].

Figure 4 shows continuous recordings of an experiment investigating the effects of pH_i on r_n. Intracellular acidosis (expected pH_i change: 7.5 to 6.5) was achieved by exposure to a solution gassed with 100% CO_2. A standard voltage-clamp pulse (−7 mV; 200 ms) was administered to cell 1 (V_1), while the nexal membrane current was monitored (I_2). For better readability, the signals during control, peak effect, and re-control were displayed on an expanded time scale. As indicated by the change in I_2 amplitude, this intervention gave rise to an increase in r_n of 13%, which was reversible after return to control solution. The alteration in r_n was *not* associated with a change in cell length.

Another set of experiments has been carried out to explore the effects of $[Ca^{2+}]_i$ on r_n. Interventions giving rise to moderate changes in $[Ca^{2+}]_i$, such as alteration of the $[Ca^{2+}]_o$ from 0.5 to 10 mmol/l, revealed no measurable changes in r_n. However, significant changes in r_n were observed with interventions producing vigorous elevations in $[Ca^{2+}]_i$. Figure 5 illustrates such an experiment in which $[Ca^{2+}]_i$ was increased by exposure to Na^+-free solution (tetramethylammonium was substituted for Na^+).

Panel A shows selected voltage (V_1) and current signals (I_2) prevailing at the nexal membrane. Panel B depicts the analysis of these records (filled circles) and others from the same experiment (open circles), plotted as nexal membrane conductance, g_n, versus time. Removal of external Na^+ produced a decrease in g_n by 25%, presumably caused by an elevation in $[Ca^{2+}]_i$ via impairment of the Na^+/Ca^{2+} exchange mechanism. Resumption of control solution gave rise to a further decrease in g_n. It is tempting to ascribe this secondary effect to Ca^{2+} release from mitochondria, the rationale being that the released Ca^{2+} was sequestered by the organelles during the Na^+-free period[1]. The change in g_n was accompanied by a sustained cell shortening.

Another set of experiments involved exposure to long-chain alcohols, such as heptanol or octanol. Short-time exposure to such substances gave rise to dramatic elevations in r_n which were readily reversible upon return to control solution. None of these interventions ever produced cell shortening, indicating that Ca^{2+} was presumably not involved.

c) Action potential transfer

Cell pairs isolated from adult ventricles represent a useful model to study the transfer of action potentials at the cellular level. Combining the voltage-clamp and current-clamp techniques, we were able to explore the propagation of the cardiac impulse in conjunction with the prevailing state of cell-to-cell coupling. The experimental protocol adopted involved 1) injection of a small rectangular current pulse to cell 1 and recording of the elicited action potential in cell 1 and the transferred action potential in cell 2, and 2) determination of r_n in the usual way (see above). The results from these experiments revealed the following pattern. In a normally coupled cell pair, exhibiting an r_n of 2–4 MΩ, the

action potential transfer occurred with no measurable delay. However, in a partially uncoupled cell pair displaying an r_n of the order of 1000 MΩ, there was no action potential transfer detectable.

Conclusions

The experiments described in this paper have been carried out on cell pairs isolated from adult rat and guinea pig ventricles by means of an enzymatic procedure. Electrical measurements indicated that the pairs of myocytes remained coupled electrically. They represent a convenient cellular preparation for investigating the electrical and pharmacological properties of the nexal membrane. Furthermore, cell pairs provide a useful model to explore the characteristics of action potential transfer at the single nexus level.

Acknowledgments. We are grateful to Dr J. Shiner for critical comments on the manuscript. Supported by the Swiss National Science Foundation (3.360–0.82; 3.253–0.85).

1 Akerman, K.E.O., and Nicholls, D.G., Physiological and bioenergetic aspects of mitochondrial calcium transport. Rev. Physiol. Biochem. Pharmac. *95* (1983) 149–206.
2 Délèze, J., and Hervé, J.C., Effect of several uncouplers of cell-to-cell communication on gap junction morphology in mammalian heart. J. Membrane Biol. *74* (1983) 203–215.
3 De Mello, W.C., Effect of intracellular injection of calcium and strontium on cell communication in heart. J. Physiol. Lond. *250* (1975) 231–245.
4 De Mello, W.C., Cell-to-Cell communication in heart and other tissues. Progr. Biophys. molec. Biol. *39* (1982) 147–182.
5 Imanaga, I., Cell-to-cell coupling as revealed by diffusional studies. Experientia *43* (1987) 1080–1083.
6 Isenberg, G., and Klöckner, U., Calcium tolerant ventricular myocytes prepared by preincubation in a 'KB medium'. Pflügers Arch. *395* (1982) 6–18.
7 Jongsma, H.J., Rook, M.R., and van Ginneken, A.C.G., The conductance of single gap junctional channels between rat neonatal heart cells. J. Physiol. Lond. *382* (1987) 134.
8 Maurer, P., and Weingart, R., Cell pairs isolated from adult guinea pig and rat hearts: Effects of $[Ca^{2+}]_i$ on nexal membrane resistance. Pflügers Arch. *409* (1987) 394–402.
9 Metzger, P., and Weingart, R., Electrical current flow in cell pairs isolated from adult rat hearts. J. Physiol. Lond. *366* (1985) 177–195.
10 Reber, W.R., and Weingart, R., Ungulate cardiac Purkinje fibres: the influence of intracellular pH on the electrical cell-to-cell coupling. J. Physiol. Lond. *328* (1982) 87–104.
11 Sakmann, B., and Neher, E., Single-channel Recording. Plenum Press, New York 1983.
12 Stewart, J.M., and Page, E., Improved stereological techniques for studying myocardial cell growth; Application to external sarcolemma, T-system, and intercalated disks of rabbit and rat hearts. J. Ultrastr. Res. *65* (1978) 119–134.
13 Tsien, R.W., Calcium channels in excitable cell membranes. A. Rev. Physiol. *45* (1983) 341–358.
14 Veenstra, R.D., and DeHaan, R.L., Single gap junctional channel activity in embryonic chick heart cells. Biophys. J. *49* (1986) 343a.
15 Weidmann, S., The electrical constants of Purkinje fibres. J. Physiol. Lond. *118* (1952) 348–360.
16 Weidmann, S., Electrical constants of trabecular muscle from mammalian heart. J. Physiol. Lond. *210* (1970) 1041–1054.
17 Weingart, R., Electrical properties of the nexal membrane studied in rat ventricular cell pairs. J. Physiol. Lond. *370* (1986) 267–284.
18 Wojtczak, J.A., Electrical uncoupling induced by general anesthetics: a calcium-independent process?, in: Gap Junctions, pp. 167–175. Eds M.V.L. Bennett and D.C. Spray. Cold Spring Harbor Laboratory, Cold Spring Harbor 1985.

0014-4754/87/101091-04$1.50 + 0.20/0

Full Papers

Metabolic iteration, evolution and cognition in cellular proliferation

E. Cervén

Faculty of Pharmaceutical Sciences, University of Tokyo, Bunkyo-ku, Tokyo 113 (Japan), 5 February 1987

Summary. A model for cellular proliferation is described according to which proliferation ensues when metabolism evolves towards commitment to DNA synthesis, and inhibition of proliferation occurs when enzymic interactions are iterated within a few metabolic pathways, another limiting factor being the supply of metabolites. The model successfully describes cellular growth and division as a 'cognitive process' based on interaction within enzymic elements and the genome, and affords an explanation in these terms of some empirical phenomena which have previously been understood only as isolated observations.
Key words. Cognitive processes; metabolism; evolution; biomathematical models; cell proliferation; cell growth.

Introduction

No simple model to explain the observed relationships between cell volume, cell mass, protein synthesis, metabolism, cellular morphology, and cell proliferation has so far been presented, although correlations between these entities have been amply investigated. For example, a correlation exists between the frequency of cell division and growth of cell mass, cell volume and cell surface area per unit time[1–6]. This correlation tends to be straightforwardly linear, i.e. the cells maintain their size under permissive nutritive conditions, while under excessive or deficient nutritive conditions[7,8] or during morula formation in embryogenesis, the timing of the determination of size may lag one or more cell generations. Both commitment to DNA synthesis[9,10] and subsequent metabolic evolution[7] tend to be probabilistic events. There is also a correlation between cell division and various metabolic rates, such as transport of metabolites[11–17], Ca^{2+}-entry into the cell[9,18], Na^+-entry[19], Na^+K^+-pump activity[19–21], Na^+H^+-exchange with cytoplasmic alkalinization[22–24] and phosphoinositide turnover[25–27]. Other mitogenic events which do not themselves belong to the category of changes of flux include e.g. binding to the cell surface of growth factors[22,28–30] or other specific ligands[20,21] and protein kinase C-activa-